Metabolism Clinical and Experimental 94 (2019) 1–8

Contents lists available at ScienceDirect

Metabolism Clinical and Experimental

journal homepage: www.metabolismjournal.com

Basic Science

LncRNA MEG3 functions as a ceRNA in regulating hepatic lipogenesis by competitively binding to miR-21 with LRP6

Peng Huang [a,b,1], Fei-zhou Huang [a,1], Huai-zheng Liu [c], Tian-yi Zhang [c], Ming-shi Yang [c], Chuan-zheng Sun [c,*]

[a] Department of General Surgery, The Third Xiangya Hospital, Central South University, 138 Tongzipo Road, Changsha 410013, China
[b] Department of General Surgery, Xiangya Hospital, Central South University, No.87 Xiangya Road, Changsha 410008, China
[c] Emergency Department, The Third Xiangya Hospital, Central South University, 138 Tongzipo Road, Changsha 410013, China

ARTICLE INFO

Article history:
Received 31 October 2018
Accepted 30 January 2019

Keywords:
Non-alcoholic fatty liver disease
Long non-coding RNA
MEG3
miR-21
LRP6
Lipid metabolism

ABSTRACT

Background: Hepatic lipogenesis dysregulation is essential for the development of non-alcoholic fatty liver disease (NAFLD). Emerging evidence indicates the importance of the involvement of long non-coding RNAs (LncRNAs) in lipogenesis. However, the specific mechanism underlying this process is not clear.
Objective: This study aimed to investigate the functional implication of LncRNA MEG3 (MEG3) in fatty degeneration of hepatocytes and in the pathogenesis of NAFLD.
Methods: The expression of MEG3 was analysed in in vitro and in vivo models of NAFLD, which were established by free fatty acid (FFA)-challenged HepG2 cells and high-fat diet-fed mice, respectively. Endogenous MEG3 was overexpressed by a specific pcDNA3.1-MEG3 to evaluate the regulatory function of MEG3 on triglyceride (TG)- and lipogenesis-related genes. Bioinformatic analysis was used to predict the target genes and binding sites, and the targeted regulatory relationship was verified with a dual luciferase assay. Finally, the possible pathway that regulates MEG3 was also evaluated.
Results: We found that the downregulation of MEG3 in vitro and in vivo models of NAFLD was negatively correlated with lipogenesis-related genes and that overexpression of MEG3 reversed FFA-induced lipid accumulation in HepG2 cells. miR-21 was upregulated in the FFA-challenged HepG2 cells and was physically associated with MEG3 in the process of lipogenesis. Our mechanistic studies demonstrated that MEG3 competitively binds to miR-21 with LRP6, followed by the inhibition of the mTOR pathway, which induces intracellular lipid accumulation.
Conclusion: Our data are the first to document the working model of MEG3 functions as a potential hepatocyte lipid degeneration suppressor. MEG3 helps to alleviate lipid over-deposition, probably by binding to miR-21 to regulate the expression of LRP6. Our results suggest the potency of MEG3 as a biomarker for NAFLD and as a therapeutic target for treatment.

1. Introduction

The incidence of non-alcoholic fatty liver disease (NAFLD) has increased drastically in recent years, which poses a serious threat to public health worldwide [1–3]. Therefore, timely intervention of NAFLD is of critical importance for alleviating the public health burden. The treatment for NAFLD consists of lifestyle intervention and pharmacological therapy. However, most drugs currently used have serious side effects, such as weight gain and increased mortality [4]. It is clear that the main cause of NAFLD is fat being over-deposited in the liver, and NAFLD is associated with obesity, insulin resistance, and metabolic syndrome [5,6]. Besides, there is increasing evidence that the dysregulation of non-coding RNAs may result in abnormal lipid metabolism, which contributes to the development of NAFLD [7], however, the underlying mechanism remains unclear.

Long non-coding RNAs (LncRNA) are a group of non-coding intracellular RNA molecules that are >200 nucleotides in length [8]. LncRNAs regulate gene expression indirectly via transcriptional regulation, posttranscriptional modification, and modulation of microRNA (miRNA) activities [9]. Emerging evidence has revealed that LncRNAs function as important contributors to biological processes underlying the pathophysiology of NAFLD [10]. In our previous study, a systematic analysis was

Abbreviations: NAFLD, Non-alcoholic fatty liver disease; LncRNAs, long non-coding RNAs; miRNA, microRNA; MEG3, maternally expressed gene 3; GTL2, gene trap locus 2; EMT, epithelial-mesenchymal transition; FFA, free fatty acid; NC, negative control; TG, triglycerides; ceRNAs, competing endogenous RNAs; PDCD4, programmed cell death 4; LRP6, low-density lipoprotein receptor-related protein 6; HFD, high-fat diet; SCD, standard chow diet; HE, Haematoxylin-eosin; SREBP1, sterol regulatory element-binding protein 1; LXRa, liver X receptor alpha; ChREBP, carbohydrate-responsive element-binding protein; SCD1, stearoyl CoA desaturase 1; ACC, acetyl CoA carboxylase; MEG3-WT, wild-type MEG3; MEG3-MUT, mutant MEG3; MREs, miRNA response elements; L-PK, liver-pyruvate kinase; LXRs, liver X receptors.

* Corresponding author.
E-mail address: sunchuanzheng@csu.edu.cn (C. Sun).

[1] These authors contributed equally to this work.

https://doi.org/10.1016/j.metabol.2019.01.018
0026-0495/

performed to detect the expression of LncRNAs in NAFLD samples, and we found that LncRNA MEG3 (maternally expressed gene 3, MEG3) levels were significantly decreased in liver tissues of NAFLD patients [11]. MEG3 also known as gene trap locus 2 (GTL2), is an imprinted gene located on chromosome 14q32.3 in humans that participates in chronic liver diseases and various types of human cancers [12,13]. It has also been reported that MEG3 can suppress fatty acid deposition by regulating miR-140 [14]. However, the role of MEG3 in fat Metabolism, and how this may modulate NAFLD remain to be clarified.

In recent years, a new regulatory mechanism has emerged, demonstrating that coding- and non-coding RNAs can regulate each other by competing for shared miRNAs, which has been demonstrated in a variety of human diseases [15]. Competing endogenous RNAs (ceRNAs), also called natural microRNA sponges, are endogenous coding or non-coding transcripts including circular RNAs, pseudogenes, and LncRNAs that share sequences with common microRNAs [15]. MEG3 functions as a ceRNA and competes with programmed cell death 4 (PDCD4) mRNA for direct binding to miR-21, which has been widely demonstrated in the process of ischaemic neuronal death [16]. Similarly, it was also demonstrated that MEG3 inhibits the Hh-mediated epithelial-mesenchymal transition (EMT) process in liver fibrosis via the SMO protein and miR-21 [12]. Nevertheless, it is not clear whether MEG3 functions as a ceRNA by competing for binding to miRNAs in the development of NAFLD.

The present study aimed to investigate the functional implication of MEG3 in fatty degeneration of hepatocytes and in the pathogenesis of NAFLD. Our data show that the expression of MEG3 was downregulated in hepatocytes with lipid degeneration and negatively related to lipogenesis-related genes. Using bioinformatics analysis and specific siRNAs we delineated the functional interactions among MEG3, miR-21, and low-density lipoprotein receptor-related protein 6 (LRP6) in NAFLD. We further confirmed that miR-21 facilitates lipid degeneration by modulating lipogenesis-related gene expression. Moreover, MEG3 competed with LRP6 mRNA for binding to miR-21 and contradicted the inhibitory effects of miR-21 on the LRP6-activated AKT/mTOR signalling pathway to regulate lipid metabolism. These findings indicate that LncRNA MEG3 functions as a ceRNA for miR-21 to regulate LRP6 expression during liver lipid deposition, which may inform new therapeutic strategies for NAFLD.

2. Materials and Methods

2.1. Mouse Model of NAFLD

The mouse model of NAFLD was developed following previously reported protocols [2]. A total of 12 C57BL/6 mice (males, 8 weeks old) were purchased from SJA Laboratory Animal Corp (Changsha, China) and weighed approximately 18 g each. The mice were divided into two groups ($N = 6$ each) and were fed a high-fat diet (HFD) or a standard chow diet (SCD) for 8 weeks to establish a mouse NAFLD model. The body weights of the mice were monitored weekly. All animal experimental procedures followed the guidelines stipulated by the Research Ethical Committee of Laboratory Animal Center, Xiangya Medical School, Central South University.

2.2. Cell Culture and Treatment

Human hepatocellular carcinoma cell line HepG2 (ATCC, US) was cultured in a humidified CO_2 chamber at 37 °C using DMEM (Gibco, US) containing penicillin, streptomycin (Invitrogen, US) and 10% foetal bovine serum (FBS) (Gibco, US). Cells were assigned to the control or free fatty acid (FFA, containing oleic acid and palmitic acid at a 2:1 volume ratio) treatment groups. In the latter group, cells were treated with gradient concentrations of FFA (0.25, 0.5, 1 and 2 mM) for 24 h and were then used for further assays.

2.3. Oil-Red O Staining

As previously described [17], cultured HepG2 cells and liver tissues were tested for lipid droplet formation using Oil-Red O staining. HepG2 cells were placed on a coverslip, washed in PBS, and then fixed in 10% formalin for 5 min. For liver tissues, formalin-fixed and paraffin-based slices were de-waxed and re-hydrated. Samples were washed briefly in isopropanol and stained with 0.5 g Oil-Red O stain for 30 min. Stained cells were washed in distilled water. Samples were then counter-stained with haematoxylin for 1 min and then observed under a bright field microscope.

2.4. Haematoxylin-Eosin (HE) Staining

HE staining was performed to examine liver tissue morphology following standard protocols. In brief, the live tissues were fixed intratracheally with 4% paraformaldehyde in phosphate buffer and were embedded in paraffin. Sections (4 μm) were stained with haematoxylin (5%) for 10 min. Tissue slices were first rinsed in distilled water, acidified and then stained in eosin for 5 min. After dehydration and coverslip mounting, tissue slices were observed under a bright field microscope.

2.5. MTT Assay

An MTT assay was employed to quantify the relative viability and proliferation of HepG2 cells from all groups. The test procedures followed those of previously reported studies [18]. In brief, cells were seeded into 96-well plates for 24 h and cultured in serum-free medium. After treatment, 20 μL of MTT solution (5 mg/mL) was added followed by 4 h of incubation, and cells were suspended in DMSO. Absorbent values were measured at 570 nm, and the proliferation rate was calculated as $(A_{Treatment} - A_{Control})/A_{Control} \times 100\%$.

2.6. Triglyceride Assay

Triglyceride (TG) levels were measured by a TG kit (Nanjing, China). The values obtained were normalized to total protein concentrations. The intracellular TG content was expressed as mmol/g protein. Protein concentrations were measured using the BCA method.

2.7. Cell Transfection

A MEG3 sequence was synthesized and sub-cloned into transfection plasmid to generate recombinant vector pcDNA3.1-MEG3 (described as MEG3 in figures). The control group was transfected with an empty pcDNA3.1 plasmid (described as pcDNA3.1 in figures). miR-21 inhibitor, miR-21 mimics and negative control (NC) were synthesized by GenePharma (Shanghai, China). Sequences were as follows [19]: miR-21 inhibitor: 5′-UCAACAUCAGUCUGAUAAGCUA-3′; miR-21 mimic: 5′-AACAUCAGUCUGAUAAGCUAUU-3′; negative control (NC), 5′-CAGU ACUUUUGUGUAGUACAA-3′. We purchased specific siRNAs for human LRP6 (sc-37233) from Santa Cruz Biotechnology (Shanghai, China). The specific plasmids were transfected into cells using Lipofectamine™ 2000 (Invitrogen, US) as described previously [20].

2.8. Dual Luciferase Reporter Assay

A dual luciferase reporter assay was employed to examine the binding activity between MEG3 and miR-21 and between miR-21 and LRP6 following established protocols in HepG2 cells [21]. First, we constructed dual-luciferase reporter gene plasmids, which were ligated to both wild-type and mutant forms of MEG3 or LRP6 gene coding sequences. In brief, HepG2 cells from all groups were transfected with a pGL3-Luc plasmid containing candidate binding elements, including MEG3 or LRP6 gene fragments linked to a firefly luciferase neo expression vector, using the approaches mentioned above. After transfection,

Table 1
Primers used for qRT-PCR analysis.

Genes	Primer sequences (5′-3′)
MEG3	F: 5′-CCATCACCTGGATGCCTACG-3′ R: 5′-GGGAATAGGTGCAGGGTGTC-3′
miR-21	F: 5′-CGCGCTAGCTTATCAGACTGA-3′ R: 5′-GTCGTATCCAGTGCAGGGTCCGAGGTATT CGCACTGGATACGACTCAACA-3′
LRP6	F: 5′-GGGAATAGGTGCAGGGTGTC-3′ R: 5′-GAAGGGAACCTTTAACCACTGC-3′
SREBP1	F: 5′-GGAGCCATGGATTGCACTTTCG-3′ R: 5′-GCTCAGGAAGGCTTCAAGAGAG-3′
LxRa	F: 5′-GCTTCTGGAGACATCTCGGAGG-3′ R: 5′-GAGTTGCAGCTCATTCATGGCC-3′
ChREBP	F: 5′-GTCATCCACAGCGGTCACTTC-3′ R: 5′-GTCTCTGCAGAGCAGCTTGAG-3′
SCD1	F: 5′-CTTGCGATATGCTGTGGTGC-3′ R: 5′-AAGTTGATGTGCCAGCGGTA-3′
ACC1	F: 5′-CAAGGTCAGCTGGTCCACATG-3′ R: 5′-CAAGGTCAGCTGGTCCACATG-3′
FAS	F: 5′-TATGAAGCCATCGTGGACGG-3′ R: 5′-TATGAAGCCATCGTGGACGG-3′
U6	F: 5′-CTCGCTTCGGCAGCACA-3′ R: 5′-AACGCTTCACGAATTTGCGT-3′
β-Actin	F: 5′-CCTCGCCTTTGCCGATCC-3′ R: 5′-GGATCTTCATGAGGTAGTCAGTC-3′

HepG2 cells were measured for *Renilla* luciferase activity using the Dual Luciferase Assay Kit (Promega, USA) according to the manufacturer's instructions. Firefly and *Renilla* luciferase activities were measured by a plate reader (NEO, Bio-Tek, USA) and normalized to *Renilla* luciferase data.

2.9. RNA Extraction and qRT-PCR

Gene expression in cultured HepG2 cells and mouse liver tissues were measured by quantitative real-time PCR (qRT-PCR) as previously described [22]. In brief, cells were collected by centrifugation, and total RNA was extracted and prepared for cDNA using the TaqMan Gene Expression Kit (Applied Biosystems, US) following the manufacturer's instructions. Quantitative real-time PCR was performed using specific primers targeting MEG3, miR-21, LRP6, SREBP1, LXRa, ChREBP, SCD1, ACC and FAS on a Step One Plus real-time PCR system (Applied Biosystems, US). PCR conditions were as follows: 95 °C for 10 min, followed by 45 cycles of 95 °C for 15 s and 60 °C for 1 min. Ct values were calculated, and the relative expression level was quantified by the $2^{-\Delta\Delta Ct}$ approach using β-actin as the housekeeping gene. Each sample was tested in triplicate for statistical analysis. The primers used in this study are provided in Table 1.

2.10. Western Blotting

Total proteins were extracted from cultured cells and liver tissues. In brief, RIPA buffer with protease inhibitors was used to lyse cells, followed by centrifugation at 14,000*g* for 10 min. The proteins were separated by SDS-PAGE and then transferred onto PVDF membranes. The membrane was then incubated with primary antibodies (targeting LRP6, AKT, p-AKT, mTOR, and p-mTOR, all at 1:1500 dilutions, from Cell Signaling, US) at 4 °C overnight. ECL chromogenic reagent was then used to develop the membrane, which was then visualized under a chemiluminescence system (Bio-Rad, US). The relative expression level was calculated by comparing integrated grey values of target proteins to the control bands as previously described [23].

2.11. Statistical Analysis

All data were included for statistical analyses using GraphPad Prism 7.0. Unpaired Student's *t*-test (two-tailed) was used for the comparison between unpaired two-groups. One-way analysis of variance (ANOVA) followed by Bonferroni test was applied for multi-group data comparison. Bar graphs were presented as means ± s.d. The difference was considered statistically significant at $P < 0.05$.

3. Results

3.1. Downregulation of MEG3 in Hepatocytes with Lipid Degeneration in Liver Tissues and the Negative Correlation with Lipogenesis-Related Genes

Our previous study suggested that MEG3 was significantly decreased in liver tissues of NAFLD patients [11].To provide further in vivo evidence, we generated a NAFLD mouse model using the HFD feeding method. Compared to the SCD group, the HFD-fed mice showed significantly more rapid body weight increases (Fig. 1A). HE staining revealed

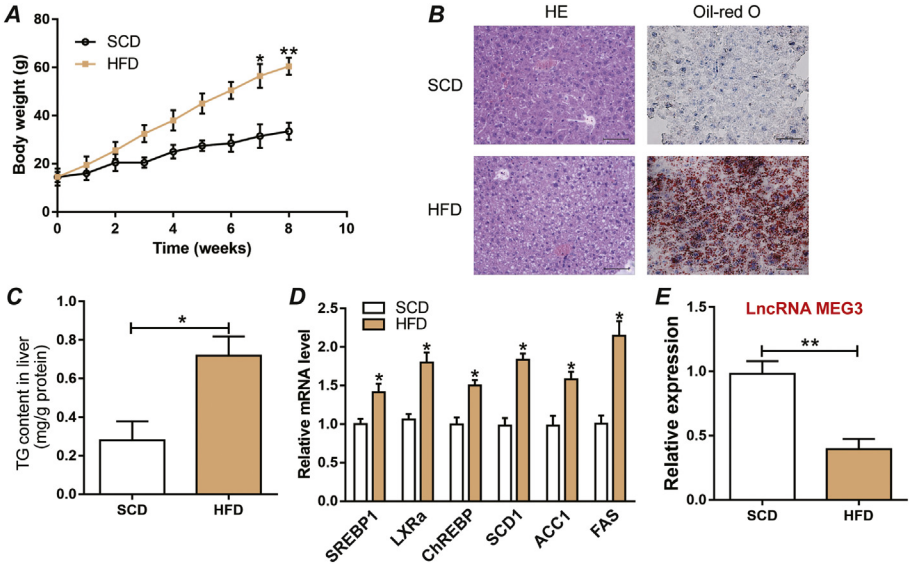

Fig. 1. Downregulation of LncRNA MEG3 in the liver tissues of HFD-fed NAFLD mice. (A) Body weight growth curves of SCD- and HFD-fed mice. (B) HE staining (left panels) shows general tissue morphology of mouse livers between SCD and HFD groups; Oil-red O staining shows prominent lipid deposition in the HFD mice (right panels). (C) TG levels in the liver tissues. (D) qRT-PCR shows the mRNA levels of lipogenesis-related genes, including SREBP1, LXRa, ChREBP, SCD1, ACC1 and FAS. (E) Relative expression levels of MEG3 between SCD- and HFD-fed mice. Data are shown as mean ± s.d., $n = 6$. The data statistical significance is assessed by Student's *t*-test, $^{*}P < 0.05$, $^{**}P < 0.01$.

notable changes in liver tissues in the HFD group, including enlarged hepatocyte volume, dispersion of lipid vacuoles, and compression of liver sinusoid (Fig. 1B). Oil-Red O staining showed prominent lipid droplet deposition in the HFD group compared to that of the SCD group (Fig. 1B). Consistent with these findings, TG levels were also significantly higher in HFD-fed mice (Fig. 1C). Furthermore, we also found elevated levels of lipogenesis genes, including SREBP-1, LXRa, ChREBP, SCD1, ACC1 and FAS, in the HFD mice (Fig. 1D). These observations demonstrated the successful generation of the NAFLD mouse model. As expected, the expression of MEG3 was significantly decreased in the liver tissues of the HFD group (Fig. 1F), which showed a negative correlation with lipogenesis-related genes.

3.2. Overexpression of MEG3 Reversed FFA-Induced Lipid Accumulation in HepG2 Cells

To establish the role of MEG3 in lipid accumulation, we treated HepG2 cells with palmitate to mimic fatty acid overload conditions. Our results showed significant lipid deposition in the FFA-treated group and deterioration with higher FFA concentrations (Fig. 2A), which resulted in gradually suppressed cell viability in a dose-dependent manner (Fig. 2B). Elevated TG levels demonstrated the successful generation of the NAFLD cell model in a dose-dependent manner (Fig. 2C). Using qRT-PCR, FFA treatment was found to suppress MEG3 expression in HepG2 cells in a dose-dependent manner (Fig. 2D).

To identify whether MEG3 was involved in the effect of palmitate on lipid accumulation, HepG2 cells were transfected with pcDNA3.1-MEG3 (described as MEG3 in figures). pcDNA3.1-MEG3 efficiently increased the expression of MEG3 in HepG2 cells (Fig. 2E). Notably, overexpression of MEG3 showed a trend to lower FFA-induced lipid accumulation in HepG2 cells (Fig. 2F). Similar results of intracellular levels of TG were also observed (Fig. 2G). Furthermore, using a qRT-PCR assay, we found that FFA treatment significantly elevated the expression levels of all six lipogenesis related genes (Fig. 3A–F). Since the expression of MEG3 in hepatocytes was negatively related to lipogenesis-related genes, we also investigated the role of MEG3 on those genes. Consistently, no matter with or without FFA treatment, overexpression of MEG3 effectively reduced the expression levels of lipogenesis-related genes (Fig. 3A–F).

3.3. MEG3 Is Physically Associated with miR-21 in the Process of Lipogenesis

Since miR-21 has been reported as the downstream effector of MEG3 [24], we further investigated the correlation between MEG3 and miR-21. Sequence analysis and an open online database, lnCeDB, provided the putative binding sites between MEG3 and miR-21 (Fig. 4A). Subsequently, we constructed luciferase reporters containing the wild-type MEG3 (MEG3-WT) or mutant MEG3 (MEG3-MUT). We also overexpressed or knockdowned the expression of miR-21 via a miR-21 mimic or a miR-21 inhibitor. Compared to the control, the miR-21 mimic and miR-21 inhibitor significantly reduced or increased the luciferase reporter activities of the MEG3-WT reporter but not those of the MEG3-MUT reporter (Fig. 4B), suggesting that MEG3 was physically associated with miR-21 via these sites.

To further validate the direct interaction between miR-21 and MEG3, we detected the expression of miR-21 and MEG3 in HepG2 cells over-expressing MEG3 or HepG2 cells that were transfected with miR-21 mimics. We found significantly decreased miR-21 expression levels in HepG2 cells after MEG3 over-expression (Fig. 4C). In addition, we observed a dose-dependent elevation in miR-21 expression in HepG2 cells treated with FFA (Fig. 4D). After treatment with the miR-

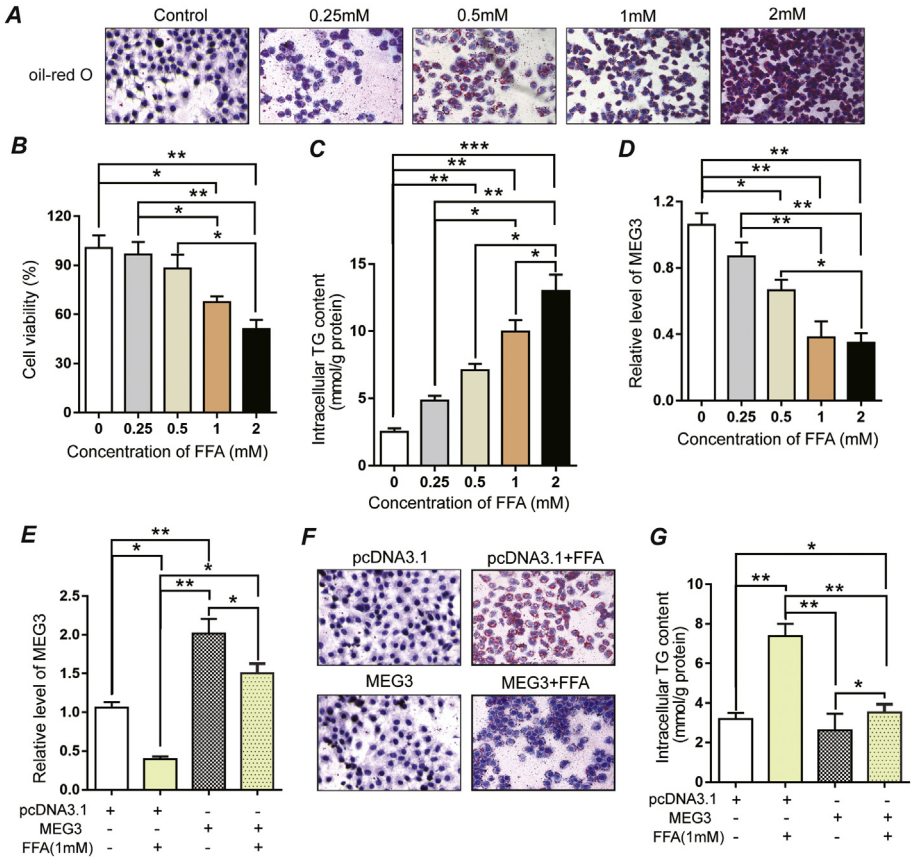

Fig. 2. Overexpression of MEG3 reversed palmitate-induced lipid accumulation in HepG2 cells. HepG2 cells were treated with different doses of FFA ranging from 0 to 2 mM, (A) Oil-Red O staining shows the lipid deposition; (B) the viability of HepG2 cells was detected by an MTT assay; (C) TG levels in HepG2 cells; (D) qRT-PCR shows MEG3 expression in HepG2 cells. HepG2 cells were treated with FFA (1 mM) plus transfected with pcDNA3.1-MEG3 (described as MEG3), (E) qRT-PCR shows the relative expression of MEG3; (F) Oil-Red O staining shows lipid deposition in HepG2 cells; (G) TG levels in HepG2 cells. Data are shown as means ± s.d., $n = 3$, $^{*}P < 0.05$, $^{**}P < 0.01$, $^{***}P < 0.001$, ANOVA test.

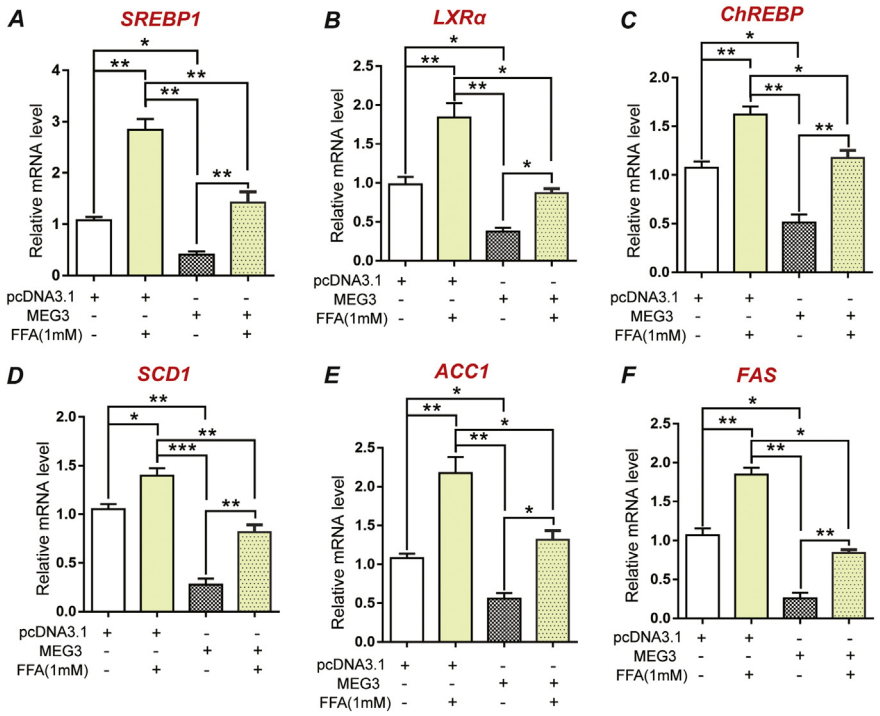

Fig. 3. Upregulation of MEG3 inhibits lipogenesis-related gene expression in HepG2 cells. HepG2 cells were treated with FFA (1 mM) plus transfected with pcDNA3.1-MEG3 (described as MEG3), qRT-PCR shows the relative mRNA level of (A) SREBP1, (B) LXRa, (C) ChREBP, (D) SCD1, (E) ACC1, and (F) FAS. Data are shown as means ± s.d., $n = 3$, $^{*}P < 0.05$, $^{**}P < 0.01$, $^{***}P < 0.001$, ANOVA test.

21 mimic or inhibitor, we found an inverse correlation between MEG3 and miR-21 expression levels (Fig. 4E), which supported that miR-21 is a MEG3-targeting miRNA.

3.4. miR-21 Is Required for FFA-Induced Intracellular Lipogenesis

To investigate the function of miR-21 in the process of lipogenesis, we detected the expression of six lipogenesis-related genes in FFA-challenged HepG2 cells transfected with a miR-21 mimic or inhibitor. We found that FFA treatment significantly elevated the expression levels of all six of these genes, which was significantly weakened by the miR-21 inhibitor and enhanced by the miR-21 mimic (Fig. 5A–E). These results suggested that miR-21 mediates FFA-induced intracellular lipid accumulation.

3.5. LRP6 Is the Direct Target of miR-21 and Is Required for miR-21-Induced Intracellular Lipid Accumulation

To identify the target of miR-21 that is responsible for the observed increase in lipid production, we predicted the target gene of miR-21 using the TargetScan program. LRP6 is a direct target of miR-21 and plays important roles in metabolic regulation, specifically in the nutrient-sensing pathway [25]. We investigated the correlation between

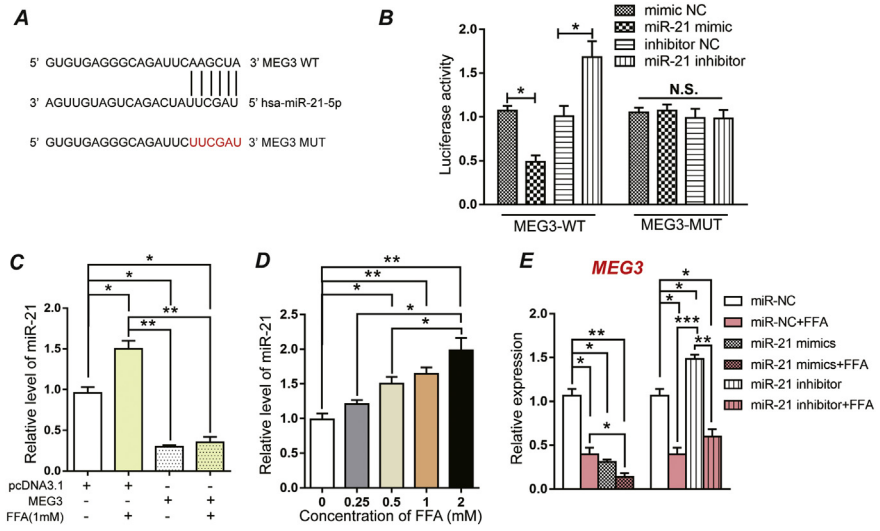

Fig. 4. The interaction of MEG3 with miR-21. (A) Predicted binding sites between miR-21 and MEG3. (B) Dual luciferase activity assay shows binding affinity between miR-21 and MEG3. (C) qRT-PCR shows the relative expression of miR-21 in HepG2 cells were treated with FFA (1 mM) plus transfected with pcDNA3.1-MEG3 (described as MEG3). (D) qRT-PCR detected the expression of miRNA-21 in HepG2 cells treated with different doses of FFA ranging from 0 to 2 mM. (E) qRT-PCR detected the expression of MEG3 in FFA-challenged (1 mM) HepG2 cells transfected with the miR-21 mimic or inhibitor. Data are shown as means ± s.d., $n = 3$, N.S. means no significance, $^{*}P < 0.05$, $^{**}P < 0.01$, $^{***}P < 0.001$, ANOVA test.

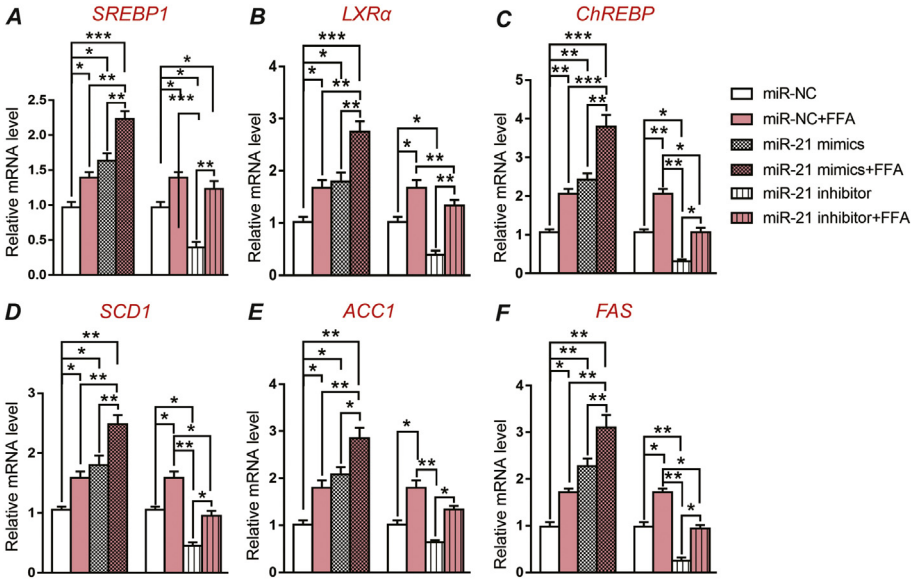

Fig. 5. Effects of miR-21 on the regulation of lipogenesis-related gene expression in HepG2 cells. HepG2 cells were treated with FFA (1 mM) plus transfected with miR-21 mimic or inhibitor, qRT-PCR detected the related mRNA level of (A) SREBP1, (B) LXRa, (C) ChREBP, (D) SCD1, (E) ACC1, and (F) FAS. Data are shown as means ± s.d., $n = 3$, $^{*}P < 0.05$, $^{**}P < 0.01$, $^{***}P < 0.001$, ANOVA test.

LRP6 and miR-21 via dual luciferase analysis. Our results indicate that miR-21 mimic and miR-21 inhibitor significantly reduced or increased the luciferase reporter activities of the LRP6-WT reporter but not those of the LRP6-MUT reporter when compared to the control (Fig. 6A). The expression of LRP6 was significantly lower in FFA-challenged HepG2 cells, demonstrating a dose-dependent relationship, which could be prevented by the miR-21 inhibitor and weakened by the miR-21 mimic (Fig. 6B, C). Next, we investigated the function of LRP6 in lipogenesis using siRNA. We found that FFA-induced intracellular lipid accumulation in HepG2 cells was significantly inhibited by siLRP6 (Fig. 6D, E).

It was reported that the activity of mTOR and the expression levels of LXR were elevated in the livers of $Lrp6_{R611C}$ mice, which resulted in the SREBP transcription factors being activated and the start of hepatic lipogenesis [26]. We therefore verified whether the mTOR pathway participated in the process of lipogenesis. In our results, the levels of phosphorylated mTOR pathway components, such as p-mTOR and p-AKT, were increased after LRP6 was silenced (Fig. 6F, G). These results suggested that LRP6 inhibits the activation of the mTOR pathway.

3.6. Overexpressed MEG3 Inhibits the Activation of the mTOR Pathway by Regulating the Expression of LRP6

Since MEG3 and LRP6 compete for binding to miR-21, we proposed that MEG3 may function as a ceRNA to regulate miRNAs with LRP6. As expected, after transfection with pcDNA3.1-MEG3, the expression of LRP6 in HepG2 cells was significantly upregulated, effectively inhibiting the activation of the mTOR pathway (Fig. 7A). Taken together these results indicate that MEG3 competes for binding to miR-21 with LRP6, which results in a weakened activation of the mTOR pathway and inhibited hepatic lipogenesis (Fig. 7B).

4. Discussion

The present study first demonstrated that excess FFAs induced intracellular lipid accumulation in hepatocytes and decreased MEG3 expression. We found that overexpression of MEG3 increased LRP6 levels and inhibited lipid accumulation. Currently, no study has revealed the direct correlation between MEG3 and NAFLD, as most studies of MEG3 have focused on its role in inhibiting tumour proliferation, including the proliferation of hepatocellular carcinoma [27]. MEG3 has been reported to be correlated with obesity in mice and has been discovered to be involved in liver fibrosis [28]; however, the function of MEG3 in the improvement of hepatic steatosis has not been studied. We thus examined MEG3 expression in both FFA-challenged HepG2 cells and HFD-fed mice. The results showed suppressed expression of MEG3 in in vitro and in vivo models, which supports the role of MEG3 in NAFLD pathogenesis. In addition, we measured TG release and lipid droplet formation in HepG2 cells after MEG3 over-expression. The results clearly showed that MEG3 upregulation suppressed lipogenesis and TG secretion, providing direct evidence for the protective role of MEG3 in the pathological process of NAFLD.

Fatty acid and fat synthesis in the liver is a highly regulated metabolic pathway, and several lipogenic genes are simultaneously regulated at the transcription level [29,30]. Emerging evidence has shown that the transcription factor ChREBP has emerged as a central regulator of lipid synthesis in the liver since it acts synergistically with SREBP to induce lipogenic genes such as ACC and FAS and is required for glucose-induced expression of the glycolytic enzyme liver-pyruvate kinase (L-PK) [31]. In general, the expression of ChREBP is regulated by liver X receptors (LXRs) [32]. Therefore, we selected SREBP1, LXRα, ChREBP, SCD1, ACC and FAS as lipogenesis-related genes, and we investigated whether MEG3 mediated the expression of these genes. In the present study, we demonstrated a negative correlation between the expression of lipogenesis-related genes and MEG3 in mouse and cell models of NAFLD. In addition, the expression of lipogenesis-related genes was significantly inhibited in HepG2 cells after increasing endogenous MEG3 levels, with or without a high FFA environment. These results provide indirect evidence that MEG3 inhibits the pathological process of NAFLD.

Further mechanistic studies indicated that LRP6 participated in the regulation of NAFLD by MEG3. LRP6 is a well-established factor regulating lipid generation and secretion [25], which is consistent with our results. The data of the present study demonstrated that decreased MEG3 levels are associated with LRP6 protein levels. The expression levels of MEG3 and LRP6 were simultaneously decreased in FFA-challenged HepG2 cells in a dose-dependent manner. In addition, dual luciferase analysis confirmed that MEG3 and LRP6 were both targets of miR-21. In this study, miR-21 was notably reduced in MEG3 over-expressing cells, and LRP6 was a target of miR-21. More importantly, increased MEG3 reduced the weakening of LRP6 in FFA-challenged HepG2 cells. Yan et al. found that MEG3 acts as a ceRNA and regulates ischaemic neuronal death by targeting the miR-21/PDCD4 signalling pathway [16], which is in accordance with our results.

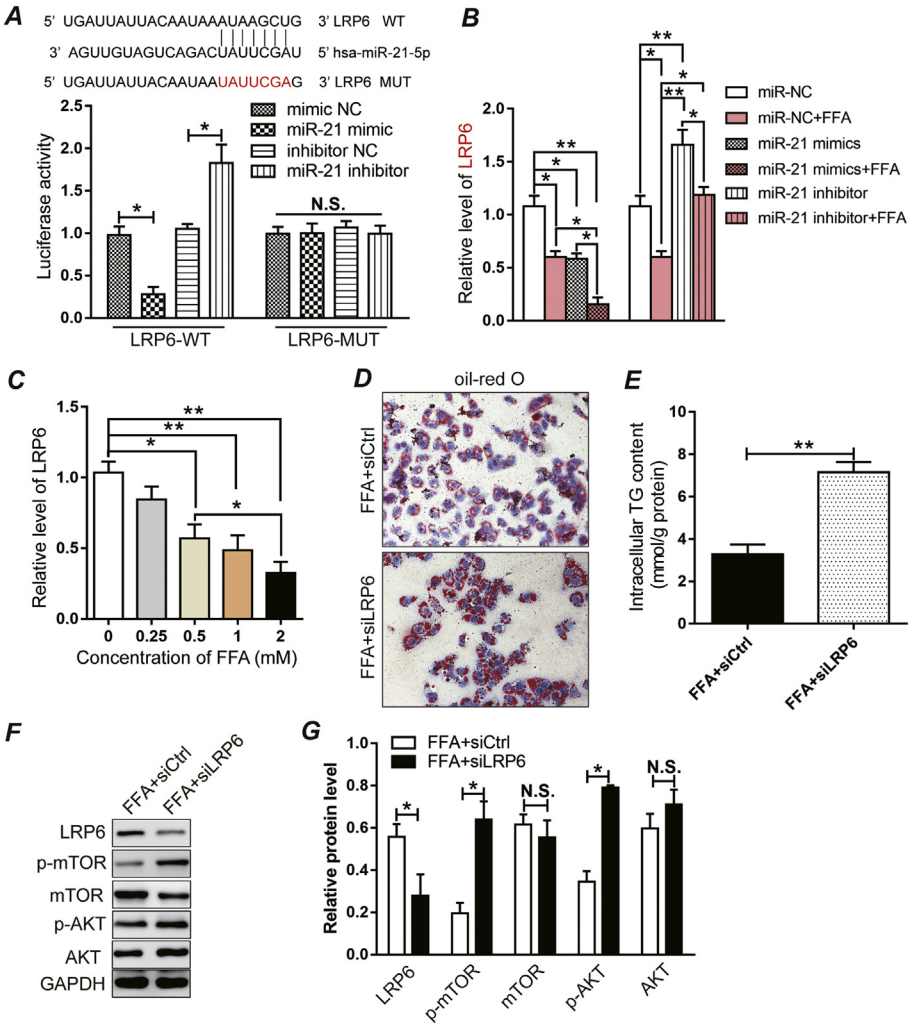

Fig. 6. LRP6 is a direct target of miR-21 and suppresses the activation of the AKT/mTOR pathway. (A) The binding sequence between miR-21 and the 3′-UTR of LRP6 and the dual luciferase activity assay shows binding affinity between miR-21 and LRP6. (B) qRT-PCR shows the relative expression of LRP6 in HepG2 cells treated with FFA (1 mM) plus transfected with miR-21 mimic or inhibitor. (C) qRT-PCR shows the relative expression of LRP6 in HepG2 cells treated with different doses of FFA ranging from 0 to 2 mM. Data are shown as means ± s.d., $n = 3$, N.S. means no significance, $^{*}P < 0.05$, $^{**}P < 0.01$, ANOVA test. After transfection with LRP6-specific silencing plasmids or negative control plasmids and treatment with 1 mM FFA, (D) Oil-Red O staining shows the lipid deposition; (E) TG levels in HepG2 cells; (F) Western-blot shows the protein expression levels of LRP6, p-mTOR, mTOR, p-AKT and AKT; (G) quantification of the protein expression levels. Data are shown as means ± s.d., $n = 3$, N.S. means no significance, $^{*}P < 0.05$, $^{**}P < 0.01$, Student's *t*-test.

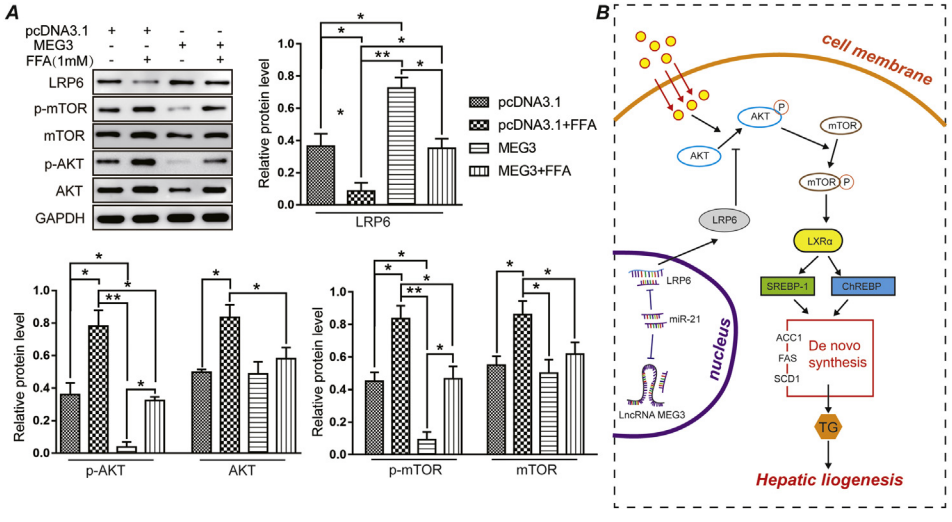

Fig. 7. MEG3 suppresses the activation of the AKT/mTOR pathway by competitively binding to miR-21 with LRP6. (A) Western blotting showing the expression of LRP6, p-mTOR, mTOR, p-AKT and AKT proteins in HepG2 cells transfected with pcDNA3.1-MEG3 and challenged with FFA (1 mM). The quantification of the protein expression levels is shown in the lower-left panels. Data are shown as means ± s.d., $n = 3$, $^{*}P < 0.05$, $^{**}P < 0.01$, ANOVA test. (B) Schematic representation of a working model in which MEG3 functions as a potential hepatocyte lipid degeneration suppressor.

In recent years, miR-21 was found to regulate TG and cholesterol metabolism [33]. For example, miR-21 was recently reported to regulate LRP6 in cultured HepG2 cells, further initiating the downstream regulation of lipid metabolic genes, including SREBP1, ACC1, LXRa and SCD1 [34]. More interestingly, NAFLD patients had elevated levels of circulating miR-21 [35], which indicated a possible correlation between NAFLD and miR-21. Downstream of miR-21, there are also various effector genes. This study is the first to identify the binding affinity between miR-21 and the 3′UTR of LRP6 gene transcripts in FFA-challenged HepG2 cells. It is well established that LRP6 regulates lipid homeostasis via the nutrient-sensing AKT/mTOR pathway, which further mediates various lipid metabolic genes. For example, in LRP6 mutant mice, the AKT/mTOR pathway was found to be activated [25,26]. In the present study, we also examined the activation levels of the mTOR pathway and found that AKT/mTOR activity was suppressed after MEG3 overexpression. Therefore, MEG3 overexpression eventually suppresses lipid degeneration via targeted suppression of miR-21 to potentiate LRP6 expression for further inhibition of the AKT-mTOR pathway.

In summary, our data identified a LncRNA MEG3-dependent lipogenesis-regulating mechanism in hepatocytes under fatty acid overload conditions. FFAs inhibited MEG3 expression upregulating miR-21, which further downregulates LRP6 expression to activate the AKT/mTOR signalling pathway, eventually leading to potentiated TG secretion and lipid degeneration. Moreover, overexpression of MEG3 strongly inhibited the expression of lipogenesis- and lipid degeneration-related genes via inhibition of miR-21 and, consequently, upregulation of LRP6; the latter of which further inhibits the AKT-mTOR signalling pathway. These results collectively suggested the potency of MEG3 as an early biomarker for NAFLD and as a drug target for disease intervention. Further assays are required in both animals and patients to elucidate the correlation between MEG3 and NAFLD disease progression.

Funding

This work was supported by the New Xiangya Talent Projects of the Third Xiangya Hospital Central South University (No. JY201618).

Acknowledgment

We would like to thank Professor Shi Chang and Professor Shirley Feng for technical assistance.

Author Contributions

PH, FZH and CZS conceived and designed the study. HL developed of the methodology. HZL, TYZ and MSY participated in the data collection and analysis. PH and CS interpreted the data and wrote the manuscript. All authors read and approved the manuscript.

Conflicts of Interest

The authors declare no conflicts of interest.

References

[1] Spengler EK, Loomba R. Recommendations for diagnosis, referral for liver biopsy, and treatment of nonalcoholic fatty liver disease and nonalcoholic steatohepatitis. Mayo Clin Proc 2015;90:1233–46.
[2] Huang P, Kaluba B, Jiang XL, Chang S, Tang XF, Mao LF, et al. Liver X receptor inverse agonist SR9243 suppresses nonalcoholic steatohepatitis intrahepatic inflammation and fibrosis. Biomed Res Int 2018;2018:8071093.
[3] Polyzos SA, Kountouras J, Mantzoros CS. Obesity and nonalcoholic fatty liver disease: from pathophysiology to therapeutics. Metabolism 2018. https://doi.org/10.1016/j.metabol.2018.11.014.
[4] Takahashi Y, Sugimoto K, Inui H, Fukusato T. Current pharmacological therapies for nonalcoholic fatty liver disease/nonalcoholic steatohepatitis. World J Gastroenterol 2015;21:3777–85.
[5] Wong VW, Wong GL, Choi PC, Chan AW, Li MK, Chan HY, et al. Disease progression of non-alcoholic fatty liver disease: a prospective study with paired liver biopsies at 3 years. Gut 2010;59:969–74.
[6] Buzzetti E, Pinzani M, Tsochatzis EA. The multiple-hit pathogenesis of non-alcoholic fatty liver disease (NAFLD). Metabolism 2016;65:1038–48.
[7] Moylan CA, Pang H, Dellinger A, Suzuki A, Garrett ME, Guy CD, et al. Hepatic gene expression profiles differentiate presymptomatic patients with mild versus severe nonalcoholic fatty liver disease. Hepatology 2014;59:471–82.
[8] Guo J, Cai H, Zheng J, Liu X, Liu Y, Ma J, et al. Long non-coding RNA NEAT1 regulates permeability of the blood-tumor barrier via miR-181d-5p-mediated expression changes in ZO-1, occludin, and claudin-5. Biochim Biophys Acta 1863;2017:2240–54.
[9] Li X, Wu Z, Fu X, Han W. lncRNAs: insights into their function and mechanics in underlying disorders. Mutat Res Rev Mutat Res 2014;762:1–21.
[10] Zhao XY, Lin JD. Long noncoding RNAs: a new regulatory code in metabolic control. Trends Biochem Sci 2015;40:586–96.
[11] Sun C, Liu X, Yi Z, Xiao X, Yang M, Hu G, et al. Genome-wide analysis of long noncoding RNA expression profiles in patients with non-alcoholic fatty liver disease. IUBMB Life 2015;67:847–52.
[12] Yu F, Geng W, Dong P, Huang Z, Zheng J. LncRNA-MEG3 inhibits activation of hepatic stellate cells through SMO protein and miR-212. Cell Death Dis 2018;9:1014.
[13] Mondal T, Subhash S, Vaid R, Enroth S, Uday S, Reinius B, et al. MEG3 long noncoding RNA regulates the TGF-beta pathway genes through formation of RNA-DNA triplex structures. Nat Commun 2015;6:7743.
[14] Li Z, Jin C, Chen S, Zheng Y, Huang Y, Jia L, et al. Long non-coding RNA MEG3 inhibits adipogenesis and promotes osteogenesis of human adipose-derived mesenchymal stem cells via miR-140-5p. Mol Cell Biochem 2017;433:51–60.
[15] Thomson DW, Dinger ME. Endogenous microRNA sponges: evidence and controversy. Nat Rev Genet 2016;17:272–83.
[16] Yan H, Rao J, Yuan J, Gao L, Huang W, Zhao L, et al. Long non-coding RNA MEG3 functions as a competing endogenous RNA to regulate ischemic neuronal death by targeting miR-21/PDCD4 signaling pathway. Cell Death Dis 2017;8:3211.
[17] Chu MJ, Hickey AJ, Tagaloa S, Zhang L, Dare AJ, MacDonald JR, et al. Ob/ob mouse livers show decreased oxidative phosphorylation efficiencies and anaerobic capacities after cold ischemia. PLoS One 2014;9:e100609.
[18] Pan Y, Wu Q, Liu R, Shao M, Pi J, Zhao X, et al. Inhibition effects of gold nanoparticles on proliferation and migration in hepatic carcinoma-conditioned HUVECs. Bioorg Med Chem Lett 2014;24:679–84.
[19] Song Y, Zuo Y, Qian XL, Chen ZP, Wang SK, Song L, et al. Inhibition of microRNA-21-5p promotes the radiation sensitivity of non-small cell lung cancer through HMSH2. Cell Physiol Biochem 2017;43:1258–72.
[20] Huang P, Mao LF, Zhang ZP, Lv WW, Feng XP, Liao HJ, et al. Down-regulated miR-125a-5p promotes the reprogramming of glucose metabolism and cell malignancy by increasing levels of CD147 in thyroid cancer. Thyroid 2018;28:613–23.
[21] Hu X, Zhang J, Jiang Y, Lei Y, Lu L, Zhou J, et al. Effect on metabolic enzymes and thyroid receptors induced by BDE-47 by activation the pregnane X receptor in HepG2, a human hepatoma cell line. Toxicol In Vitro 2014;28:1377–85.
[22] Shi B, Andrukhov O, Berner S, Schedle A, Rausch-Fan X. The angiogenic behaviors of human umbilical vein endothelial cells (HUVEC) in co-culture with osteoblast-like cells (MG-63) on different titanium surfaces. Dent Mater 2014;30:839–47.
[23] Huang P, Chang S, Jiang X, Su J, Dong C, Liu X, et al. RNA interference targeting CD147 inhibits the proliferation, invasiveness, and metastatic activity of thyroid carcinoma cells by down-regulating glycolysis. Int J Clin Exp Pathol 2015;8:309–18.
[24] Zhou X, Yuan P, Liu Q, Liu Z. LncRNA MEG3 regulates imatinib resistance in chronic myeloid leukemia via suppressing microRNA-21. Biomol Ther 2017;25:490–6.
[25] Go GW. Low-density lipoprotein receptor-related protein 6 (LRP6) is a novel nutritional therapeutic target for hyperlipidemia, non-alcoholic fatty liver disease, and atherosclerosis. Nutrients 2015;7:4453–64.
[26] Go GW, Srivastava R, Hernandez-Ono A, Gang G, Smith SB, Booth CJ, et al. The combined hyperlipidemia caused by impaired Wnt-LRP6 signaling is reversed by Wnt3a rescue. Cell Metab 2014;19:209–20.
[27] He JH, Han ZP, Liu JM, Zhou JB, Zou MX, Lv YB, et al. Overexpression of long non-coding RNA MEG3 inhibits proliferation of hepatocellular carcinoma Huh7 cells via negative modulation of miRNA-664. J Cell Biochem 2017;118:3713–21.
[28] Zhu X, Wu YB, Zhou J, Kang DM. Upregulation of lncRNA MEG3 promotes hepatic insulin resistance via increasing FoxO1 expression. Biochem Biophys Res Commun 2016;469:319–25.
[29] Wang Y, Viscarra J, Kim SJ, Sul HS. Transcriptional regulation of hepatic lipogenesis. Nat Rev Mol Cell Biol 2015;16:678–89.
[30] Polyzos SA, Mantzoros CS. Obesity: seize the day, fight the fat. Metabolism 2019. https://doi.org/10.1016/j.metabol.2018.12.011.
[31] Xu X, So JS, Park JG, Lee AH. Transcriptional control of hepatic lipid metabolism by SREBP and ChREBP. Semin Liver Dis 2013;33:301–11.
[32] Gauthier K, Billon C, Bissler M, Beylot M, Lobaccaro JM, Vanacker JM, et al. Thyroid hormone receptor beta (TRbeta) and liver X receptor (LXR) regulate carbohydrate-response element-binding protein (ChREBP) expression in a tissue-selective manner. J Biol Chem 2010;285:28156–63.
[33] Sun C, Huang F, Liu X, Xiao X, Yang M, Hu G, et al. miR-21 regulates triglyceride and cholesterol metabolism in non-alcoholic fatty liver disease by targeting HMGCR. Int J Mol Med 2015;35:847–53.
[34] Antza C, Stabouli S, Natsis M, Doundoulakis I, Kotsis V. Obesity-induced hypertension: new insights. Curr Pharm Des 2017;23:4620–5.
[35] Yamada H, Suzuki K, Ichino N, Ando Y, Sawada A, Osakabe K, et al. Associations between circulating microRNAs (miR-21, miR-34a, miR-122 and miR-451) and non-alcoholic fatty liver. Clin Chim Acta 2013;424:99–103.